project 24

DOE/BETC-3000-1
(DE81030779)
Distribution Category UC-92a

METHODS FOR DETERMINING VENTED VOLUMES DURING GAS-CONDENSATE AND OIL WELL BLOWOUTS

By

Murray F. Hawkins, Jr., *Principal Investigator*
Zaki Bassiouni
William J. Bernard
Adam T. Bourgoyne
John H. McMullan
Michael J. Veazey
Walter R. Whitehead

Coastal Petroleum Associates, Inc.
P.O. Drawer 16450-B
Baton Rouge, Louisiana 70893
504/769-1321

C. Ray Williams, *Technical Project Officer*
U.S. Department of Energy
Bartlesville Energy Technology Center
P.O. Box 1398
Bartlesville, Oklahoma 74005-1398
918/336-2400, Ext. 359

Prepared for the U.S. Department of Energy
Under P.O. No. P-B-9-3000 and
Funded by USGS/OCS Oil and Gas Operations

Date Published—September 1981

U.S. DEPARTMENT OF ENERGY

FOREWORD

When hydrocarbons are lost from a well during a blowout on federal leases, the U.S. Geological Survey (USGS) must estimate the lost volumes for purposes of establishing proper compensation. Similarly, the petroleum industry must also make estimates for use in legal defenses or settlements. This publication is a concensus of the accepted flow volume calculation methods for gas-condensate and oil well blowouts and proposes some new methods which need further definition or research.

It is probable that this publication, along with the previous report (DOE/BETC/2215-1) on gas well volume measurements, will save countless hours of research and cross-reference work for government and industry engineers. These publications should also aid the legal system by providing a reliable document authored by recognized experts.

This work was funded by the Research and Development Program for Outer Continental Shelf Oil and Gas Operations of the USGS in cooperation with Bartlesville Energy Technology Center (BETC) of the U.S. Department of Energy. BETC provided contracting, monitoring and technology transfer through its Drilling Technology Program.

John B. Gregory
Research Program Manager
OCS Oil and Gas Operations
U.S.G.S., Reston, VA

C. Ray Williams
Project Manager
Drilling and Offshore Technology
Bartlesville Energy Technology Center
U. S. Department of Energy
Bartlesville, OK

CONTENTS

		Page
Abstract.		1
1.	SCOPE OF INVESTIGATIONS	1
1.1	Introduction	1
1.2	Industry Survey	1
1.3	Gas-Condensate Well Blowout Methods	2
1.4	Oil Well Blowout Methods	3
1.5	Bleed Line Measurements	3
1.6	Cross Plot of Formation and Flow String Resistances	4
2.	MEASUREMENTS IN BLEED LINES	5
2.1	Bleed Line Flow Calculations Using Upstream Pressure	6
2.2	Illustrative Example 2.1	7
2.3	Bleed Line Flow Calculations Using Differential Pressure	9
2.4	Illustrative Example 2.2	10
2.5	Limitations and Accuracy of Bleed Line Flow Calculations	11
3.	FORMATION RESISTANCE	13
3.1	Reservoir Geometry	13
3.2	Effect of Free Gas Presence	14
3.3	Steady State Flow - No Free Gas Saturation	14
3.4	Transient Flow - No Free Gas Saturation	15
3.5	Illustrative Example 3.1	16
3.6	Flow With Free Gas Saturation Around the Wellbore	17
4.	FLOW STRING RESISTANCE	19
4.1	Flow String Resistance Calculations	19
4.2	Critical Flow	20
4.3	Flow Up Drillpipe (Illustrative Example).	21
4.4	Flow Up the Drillpipe Casing Annulus (Illustrative Example).	21
4.5	Flow Up the Casing (Illustrative Example)	28
4.6	Limitations and Accuracy of Flow String Resistance Calculations	31

CONTENTS (continued)

Page

5. CROSS PLOTS OF FORMATION AND FLOW STRING RESISTANCE 32

6. SUGGESTIONS FOR FURTHER INVESTIGATION 34

6.1 Refinements in Current Technology 34
6.2 Suggestions for New Technology 34

REFERENCES 35

FIGURES

Figure 2.1 5
Figure 2.2 5
Figure 2.3 5
Figure 2.4 8
Figure 2.5 9
Figure 3.1 13
Figure 3.2 17
Figure 4.1 23
Figure 4.2 23
Figure 4.3 24
Figure 4.4 24
Figure 4.5 26
Figure 4.6 26
Figure 4.7 27
Figure 4.8 27
Figure 4.9 29
Figure 4.10 29
Figure 4.11 30
Figure 4.12 30
Figure 4.13 31
Figure 5.1 33

TABLES

Table 2.1 8
Table 2.2 11
Table 4.1 20
Table 4.2 22
Table 4.3 25
Table 4.4 28

ABSTRACT

Several methods are presented for determining vented volumes during gas-condensate and oil well blowouts. Each method is illustrated with a numerical example. The method of crossplotting formation and flow string resistances is the only one which does not require special measurements. It is therefore applicable to cratered wells and underwater blowouts. The report includes several suggestions for investigations which might lead to better methods.

SECTION 1

SCOPE OF INVESTIGATIONS

1.1 Introduction

In October 1980 the U.S. Department of Energy published "Methods for Determining Vented Volumes During Gas Well Blowouts," by Bassiouni et al., Ref. 1.1. The same authors of that report also contracted to investigate methods which are or can be used to determine volumes of hydrocarbons lost during blowouts of gas-condensate and oil wells. They proposed to consider, where applicable, gas-condensate and oil well blowouts in the same ten categories of the gas well blowout study, namely:

1. Industry Survey
2. Material Balance Methods
3. Flow Rate Measurements with Pitot Tubes
4. Measurements in Bleed Lines
5. Extrapolation of Measured Open Flow Rates
6. Estimates from Back Pressure Tests
7. Formation Resistance
8. Flow String Resistance
9. Cross Plots of Formation and Flow Resistances
10. Suggestions for Further Investigation

Some of the methods listed above and described in Ref. 1.1 for gas well blowouts are applicable, however in some cases with limitations or caveats, to either gas-condensate or oil well blowouts, or to both. Therefore in such cases the methods of Ref. 1.1 will not be repeated in this report.

1.2 Industry Survey

The industry survey reported in Ref. 1.1 was conducted with interest in blowouts of any kind, not just gas well blowouts. The discussion of that survey therefore applies generally to gas-condensate and oil well blowouts; however not all of the methods suggested by the survey are applicable to gas-condensate and/or oil well blowouts, as discussed below.

With gas-condensate and oil well blowouts there is an additional method which may sometimes be useful and which is not applicable to gas well blowouts. This is the estimation of vented volumes of condensate or oil where appreciable portions of these liquids can be collected in surface depressions, pits or tanks. For example in the Lakeview Pool blowout in 1910, according to Sims and Frailing (Ref. 1.2) some 8,250,000 barrels of oil were captured by surface dams in 540 days of a blowing well.

For blowouts over water it is sometimes possible to make fairly reliable estimates of vented hydrocarbon liquids from areal and thickness measurements on the slicks. In the Petroleos Mexicanos' Ixtoc #1 well which blew out off Mexico June 3, 1979 (Ref. 1.3), the initial flow rate was thus estimated at 30,000 b/d. The flowrate was subsequently reduced to 20,000 b/d in July 1979 and to 10,000 b/d in August 1979 by pumping mud, metal balls, cement, and gelatin into the hole. It was estimated then that the well would dump as much as 2.9 million bbl of crude into the Bay of Campeche in a 4 month period.

1.3 Gas-Condensate Well Blowout Methods

Referring to the categories listed in Sec. 1.1, material balance methods (Item 2) are used with gas-condensate reservoirs as described for gas reservoirs in Ref. 1.1, and will not be repeated in this report. The methods do not, however, apply to retrograde reservoirs where pressures fall below their dew point pressures. In these cases the material balances are considerably more complex, and beyond the scope of these investigations.

Because of the presence of condensate liquid in the flow stream, flow rate measurements with Pitot tubes (Item 3) are not recommended for gas-condensate production. Extrapolation methods (Item 5) and estimates from back pressure tests (Item 6) can be used with gas-condensate wells as described for gas wells in Ref. 1.1.

At the time the proposal was made for these investigations it was hoped that two-phase flow correlations could be made available from unpublished sources so that measurements in bleed lines (Item 4) and calculations of flow string resistances (Item 8) could be made for gas condensate flow. These lacking, it is recommended that the methods described in Ref. 1.1 for gas flow be used, converting all condensate to its gas equivalent and treating the stream as single phase gas flow. The results using both methods will give higher gas flow rates than if two-phase flow had been accounted for in the horizontal or vertical flow strings. The difference will be small for high gas/condensate ratios, growing larger for lower gas/condensate ratios.

The calculation of formation resistance is the same as described in Ref. 1.1 for gas reservoirs. In the case of retrograde condensate reservoirs where flowing bottom hole pressures are below the reservoir fluid dew point pressure, the accumulating retrograde liquid in the vicinity of the well bore will restrict the gas flow rate. Such reductions are similar to well bore damage discussed in Ref. 1.1, and may reduce gas flow rates by as much as fifty percent. The amount of reduction however, is not amenable to reliable calculation with data usually available.

Cross plots of formation and flow string resistances (Item 9) are made as described in Ref. 1.1 for gas reservoirs. As explained above it should be remembered that flow string rates calculated assuming single phase flow are higher than actual with two-phase flow.

1.4 Oil Well Blowout Methods

Referring again to the categories of Sec. 1.1, material balance methods (Item 2), although theoretically applicable, are impractical for use in determining volumes vented during oil well blowouts, except under most favorable circumstances. Even for gas and gas-condensate reservoirs, circumstances favorable for the use of the material balance method will rarely be found. The added complexity of oil reservoir performance virtually excludes its use. A treatment of the extensive literature on material balances on oil reservoirs and their application to determining vented volumes during blowouts is beyond the scope of these investigations. In principle, the method is applied to oil well blowouts as discribed for gas well blowouts in Ref. 1.1, but it should be attempted only where circumstances are favorable, i.e., reliable pressure, PVT and reservoir data, and then only by experienced reservoir engineers.

Flow measurements with Pitot tubes (Item 3) are not applicable to two-phase flow of gas and oil. The use of flow potential tests on oil wells, the counterpart of back pressure tests on gas wells (Item 6), to estimate open flow rates are generally much less reliable than the use of gas well back pressure tests, because of the complications introduced by changing conditions of two-phase flow of gas and oil in both the reservoir and the flow string at high flow rates. Exceptions are oil wells which are produced almost unrestricted through large diameter flow strings, such as many Middle East wells where rates are several thousands of barrels of oil per day and higher.

The extrapolation of measured open flow rates (Item 5), as described for gas wells, is used in the same way with oil wells. The method requires, of course, that the flow can somehow be measured during part of the blowout period.

In view of the above, there remains for the bulk of this report only the consideration of two methods for oil well blowouts, (a) measurements in bleedlines (Item 4) and (b) the calculation and cross plot of formation and flow string resistances (Items 7, 8, and 9). A preview of these methods will follow in Secs. 1.5 and 1.6 and will be treated fully with illustrative examples in Secs. 2, 3, 4, and 5.

1.5 Bleed Line Measurements

Bleed line measurements used to determine flow rates require, of course, that the well must be under partial control, flow taking place through bleed or diverter lines installed prior to or during the blowout. Of the two techniques presented in Sec. 2., the first requires a measurement only of the pressure at some point in the line. Additional data which must be known or estimated include line length from the pressure point to the point of discharge to the atmosphere, line diameter, line temperature, gas/oil ratio, oil and gas specific gravities and water/oil ratio where water accompanies the

flow. Using one of several available multiphase, pressure loss correlations for horizontal flow, an iterative procedure requiring a computer is used to determine the oil flow rate which yields the measured upstream pressure. The second technique is similar except that here pressure taps at two points are required so as to measured the absolute pressure at either point and the differential pressure between the two points. Additional data are the same as for the first method except for line length which here is the distance between the two pressure taps. The iterative procedure is similar to that used in the first technique, finding that flow rate which predicts the measured differential pressure. The second technique is preferable in that the effects of critical flow at the point of discharge need not be considered.

1.6 Cross Plot of Formation and Flow String Resistances

Sections 3, 4, and 5 describe the determination of oil flow rates where surface pressure measurements are not available or possible. In this method the flow rates from the formation are calculated for various assumed flowing bottom hole pressures. Next, using one of several correlations which have been developed for multiphase, vertical flow, an iterative process is used to calculate flowing bottom hole pressures for a range of assumed oil flow rates. A cross plot of these two sets of data determines the flow rate with the same flowing bottom hole pressure. In addition to the several uncertainties discussed in Ref. 1.1 in using this method with gas wells, with oil wells there are added the uncertainties in using correlations which are based on measurements in pipes of smaller diameter and using flow rates considerably below those usually encountered in oil well blowouts. The correlations were developed for flow rates up to several hundreds of barrels of oil per day in production-tubing-strings of a few to several inches diameter. It is arguable that somewhat proportionally large increases in both flow rates and flow string diameters help to maintain the validity of the correlations. Further uncertainty is introduced if results obtained using different correlations are compared. In the example presented in Section 4, the flow string resistances are calculated using three different multiphase correlations.

SECTION 2

MEASUREMENTS IN BLEED LINES

Figures 2.1, 2.2, and 2.3 are diagrams of typical choke manifold assemblies recommended by the American Petroleum Institute (Ref. 2.1) for various working pressures. In addition to two or three vent lines through which flow is controlled by manual and/or remotely operated adjustable chokes, these systems contain bleed lines through which well fluids may be allowed to flow unrestricted to the atmosphere.

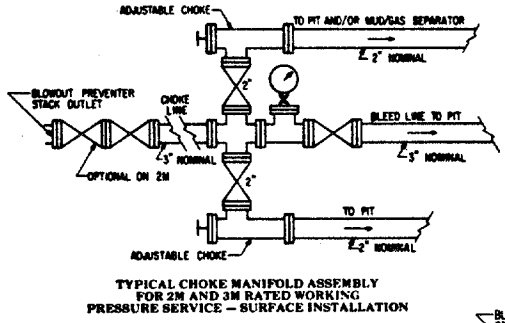

TYPICAL CHOKE MANIFOLD ASSEMBLY FOR 2M AND 3M RATED WORKING PRESSURE SERVICE – SURFACE INSTALLATION

Fig. 2.1

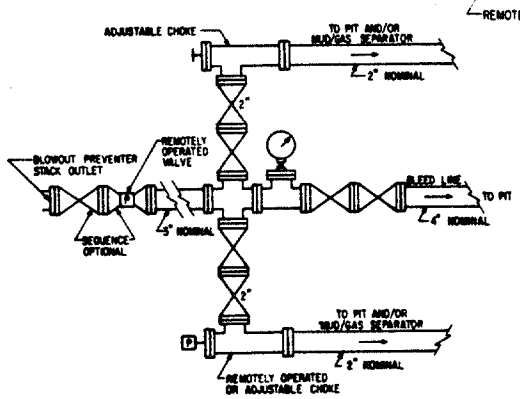

TYPICAL CHOKE MANIFOLD ASSEMBLY FOR 5M RATED WORKING PRESSURE SERVICE – SURFACE INSTALLATION

Fig. 2.2

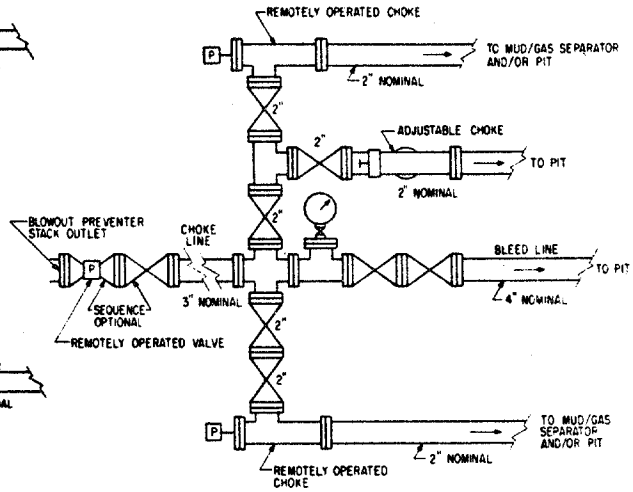

TYPICAL CHOKE MANIFOLD ASSEMBLY FOR 10M AND 15M RATED WORKING PRESSURE SERVICE – SURFACE INSTALLATION

Fig. 2.3

Bleed lines are usually straight runs of horizontal pipe, 50 to 100 feet long with a diameter at least that of the choke lines. The upstream end of the bleed line contains one or two plug or gate valves and a pressure gauge. The downstream end is open to the atmosphere. Where wells are vented or blowing out through bleed lines, it is possible to estimate the flow rate from pressure gauge readings and the length and diameter of the bleed line. This method of calculating flow rate can also be applied to diverter or blooie lines where the lines are equipped with pressure gauges.

2.1 Bleed Line Flow Calculations Using Upstream Pressure

The determination of flow rates in bleed lines during oil well blowouts is a multi-phase flow problem about the simultaneous flow of oil, gas, and water. Numerous correlations are available to predict horizontal frictional pressure losses in multiphase flow (Ref. 2.2, 2.3, 2.4, 2.5, and 2.6). This investigation utilizes the Beggs and Brill correlation described in Ref. 2.6. Because of the iterative nature of the calculations, they require computer programs incorporating many of the subroutines given in Ref. 2.6.

The possibility of critical flow must be considered where high flow rates and low pressures exist. Critical flow is defined as the point where the average velocity of the flowing fluids reaches the velocity of sound in the fluids. When this point is reached, further decrease in downstream pressure will not cause further increase in the average velocity.

In the case of flow through bleed lines, the minimum pressure and therefore the maximum velocity would occur at the outlet of the bleed line to the atmosphere. As long as the velocity at atmospheric pressure is below the velocity of sound in the fluid, critical flow does not exist, and atmospheric pressure can be used for the pressure at the outlet of the bleed line. When the exit velocity at atmospheric pressure reaches the velocity of sound in the fluid, the pressure at the point of discharge in the atmosphere is higher than atmospheric pressure. To determine this pressure, an empirical equation originally developed by Gilbert (Ref. 2.7) to predict sonic flow through chokes may be used:

$$P = \frac{10 \times Q_L \times R_P^{0.546}}{d^{1.89}} \qquad (2.1)$$

where:

P = pressure (psia)

Q_L = liquid production rate (STB/DAY)

R_P = producing gas-liquid ratio (SCF/STB)

d = pipe diameter (64th's of an inch)

The multiphase correlation of Ref. 2.6 is used to construct a plot of flow rate versus inlet pressure, measured by the gauge, using a range of assumed values of flow rate Q. Each assumed flow rate is first used to calculate the outlet pressure using Eq. 2.1. If the pressure as calculated by the equation exceeds atmospheric, the calculated pressure should be used in place of atmospheric for the discharge pressure.

To conduct the above calculations, values of water-oil ratio, gas-oil ratio, flowline temperature, oil gravity, and gas gravity must be estimated or measured. The equivalent length of any valves should be added to the length of the bleed line in calculating frictional pressure losses. The equivalent lengths of valves can be estimated from Ref. 2.8.

2.2 Illustrative Example 2.1

An oil well is vented through two fully-opened gate valves and a 50-ft, 4-in. schedule 160 bleed line. Additional data are as follows:

Line inside diameter = 3.438 in.

Absolute pipe roughness = 0.00065 in.

Gas/Oil ratio = 1000 SCF/STB

Upstream bleed line pressure = 150 psig

Flowline temperature = 180° F

Oil gravity = 35° API

Gas gravity = 0.65 (air = 1)

No water production

The equivalent length of the two gate valves is 7.45 ft (Ref. 2.8) so that the effective length for use in calculation is 57.45 ft. A computer program using the Beggs and Brill correlation described in Ref. 2.6 is now used to determine the flow rates as a function of upstream pressure. These values, together with the discharge pressures resulting from critical flow, are listed in Table 2.1. The values in Table 2.1 are plotted in Fig. 2.4, from which, for this example, the flow rate can be read directly by entering at the known upstream pressure. For this example the upstream pressure of 150 psig yields a flow rate of about 7,100 BOPD, accompanied by a gas flow of 7,100 MSCFD.

Table 2.1

Flow Rate BOPD	Discharge Pressure psig (From Eq. 2.1)	Upstream Pressure psig (Two-Phase Flow Program)
2,000	17.8	34.5
4,000	50.3	80.2
6,000	82.8	125.4
8,000	115.3	170.3
10,000	147.7	214.0

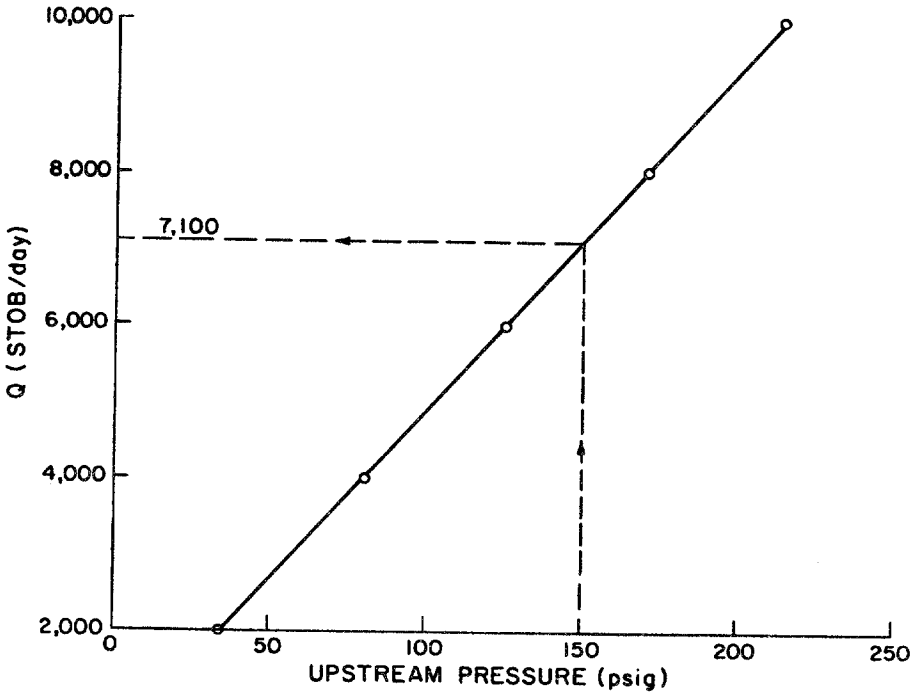

Fig. 2.4. Flow Rate as a Function of Upstream Pressure for Illustrative Example 2.1.

If the frictional losses in the bleed line are neglected, the upstream pressure can be used to estimate the flow rate. This suggests a "short cut" method of calculating maximum flow rates using the following rearranged form of Eq. 2.1:

$$Q_L = \frac{P \times d^{1.89}}{10 \times R_P^{0.546}} \qquad (2.2)$$

In the previous example for an upstream pressure of 150 psig (164.7 psia) the calculated flow rate using this "short-cut" method can be found as follows:

$$d = 3.438 \times 64 = 220 \text{ 64ths}$$

$$Q = \frac{164.7 \times 220^{1.89}}{10 \times 1000^{0.546}} = 10{,}136 \text{ BOPD}$$

This "short-cut" method results in a calculated rate 43% greater than that found using sophisticated computer programs.

2.3 Bleed Line Flow Calculations Using Differential Pressure

An alternate method would use two pipe taps located on the bleed line. The pipe taps would be fairly close to each other on a straight run of pipe. A standard differential and static pressure recorder would be used as illustrated in Fig. 2.5. This recorder measures the differential pressure between the pipe taps, i.e., the frictional loss in the bleed line between the taps. The pressure at the downstream (or upstream) pipe tap is also measured. If the downstream pressure, the pressure drop, the distance between the pipe taps, and the fluid properties are known, the flow rate can be computed.

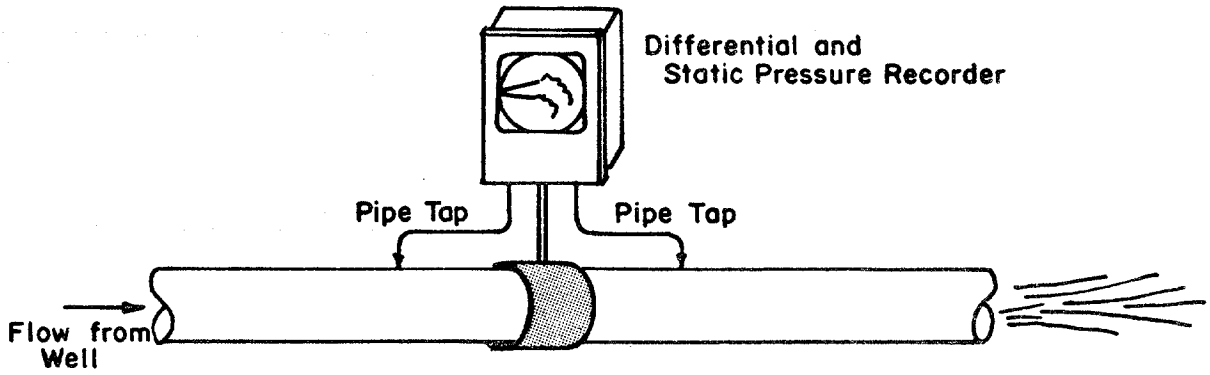

Fig. 2.5. Differential and Static Pressure Recorder for Measuring Flow Rates in Bleed Line.

These data are used in trial-and-error calculations in which an assumption is made for the flow rate. Using this flow rate, the pressure differential between the pipe taps is calculated using the Beggs and Brill correlation described in Ref. 2.6. As in the previous method the complexity of the calculation necessitates computer assistance.

The calculated differential pressure is compared with that measured by the recorder. If the calculated differential is too high, a second lower trial value for the flow rate is used to calculate a new differential pressure; or, if the calculated differential is low, a higher flow rate is used. This new differential pressure is once again compared with the measured differential, and the process is repeated until use of the trial flow rate yields the measured differential pressure, the last trial flow rate being the computed flow rate.

This technique eliminates the need to consider critical flow. This is because critical flow can only exist at the lowest pressure in the bleed line and this is at the point of discharge to the atmosphere. The pipe taps should be located upstream of the discharge in an area of subcritical flow. Unfortunately, bleed lines are not ordinarily equipped with pipe taps as described. The pipe taps, however, could be installed with hot tapping techniques. As in the previous method, values of water-oil ratio, gas-oil ratio, flow line temperature, oil gravity, and gas gravity must be estimated or measured.

2.4 Illustrative Example 2.2

An oil well is vented through a 4-in. schedule 160 bleed line. The bleed line has two pipe taps installed 10 feet apart. A recorder indicates 11.0 psi pressure differential between the pipe taps and a downstream pressure of 110 psig. Additional data are as follows:

Line inside diameter = 3.438 in.

Absolute pipe roughness = 0.00065 in.

Gas/Oil ratio = 1000 SCF/STB

Flowline Temperature = 180° F

Gas gravity = 0.65 (air = 1)

Oil Gravity = 35° API

No water production

Using the procedure described above, the differential pressures for the assumed oil flow rates can be calculated until the flow rate that yields the measured differential is found. The results of this procedure are illustrated in Table 2.2. A flow rate of about 7,400 STBO/day for Example 2.2 is indicated.

Table 2.2

Calculated Pressure Differential for Trial Flow Rates for Example 2.2

Assumed Rate STB/day	Calculated Differential psi
2,000	0.6
4,000	2.6
6,000	6.5
8,000	13.6
7,000	9.6
7,500	11.4
7,250	10.5
7,400	11.0

2.5 Limitations and Accuracy of Bleed Line Flow Calculations

Equation 2.1 was derived from data for chokes with diameter up to 9/32 in. For this purpose liquid rates can be determined with probable errors less than about 16%, as inferred from Ref. 2.7. It is not known how much larger, if any, the probable error is for pipes of several inches diameter and with much larger length to diameter ratios than for chokes. It is arguable that Eq. 2.1 is equally applicable to bleed lines, which behave as long large-diameter chokes, because their larger diameters (areas) are accompanied by correspondingly larger flow rates. Where choke liquid flow rates are in hundreds to thousands of barrels per day, bleed line rates are in the range of thousands to tens of thousands of barrels per day.

The probable errors in the frictional losses computed using the Beggs and Brill correlation is ±28% depending upon the range of some of the variables involved. As the liquid flow rate by Eq. 2.1 is directly proportional to the downstream pressure, application of the above probable errors provides upper and lower values for the downstream pressure which give upper and lower limits for the liquid flow rate. Of course, if the frictional loss is neglected, as in the short cut method, the maximum flow rate is obtained, to which the probable error of Eq. 2.1 may be applied. The error in the gauge reading is considered to be negligible compared with the uncertainties in using Eq. 2.1 and the Beggs and Brill correlations.

Because of the large volume of work involved and the limited scope of this investigation, no studies were made on variable sensitivity. Properly

done, these would involve comparative studies using the correlations of Refs. 2.2-2.5 in addition to those of Beggs and Brill (Ref. 2.6). Gas-oil ratios are likely to be unknown in many blowouts, and as the ratio enters into both Eq. 2.1 and the computation using Beggs and Brill correlations, it will considerably affect the result. Other things being the same, Eq. 2.1 indicates that the liquid flow rate for a gas-oil ratio of 1000 SCF/bbl is about one third that for a ratio of 100 SCF/bbl. As the higher gas-oil ratio will also increase the frictional loss in the bleed line, thus reducing the discharge pressure in Eq. 2.1, the reduction will be even more. Of the two suggested methods the one making use of pressure taps should yield more reasonable estimates because it eliminates the uncertainties introduced by the use of empirical Eq. 2.1.

The above calculations are limited to the case of a line of uniform cross section with no area restriction. This should usually be the case except when a valve is partially closed. A partially closed valve creates a throat. With a limited length of the line it is possible that the flow may be choked at the throat. The situation becomes somewhat more complex as supersonic flow might occur at the throat exit. Also with the valve partially closed it is hard to predict the friction losses across the valve, the cross section of the flow and the flow temperature and pressure at the throat. However, flow rates calculated assuming fully open valves are maximum estimates.

From the previous discussion it is obvious that assignment of probable errors to calculated bleed line flow rates is difficult if not impossible. It would be hard to justify probable errors of less than ±100% for the methods presented, which is to say essentially that they provide order-of-magnitude values only.

SECTION 3

FORMATION RESISTANCE

The flow rate during a blowout is controlled by formation and flow string resistances acting in series. This section discusses methods of estimating formation resistance. Section 4 discusses the determination of flow string resistance and Section 5 discusses the cross plotting of the two resistances to determine flow rate.

Formation resistance occurs as oil flows through the small, tortuous pore spaces of the reservoir rock toward the wellbore. The relationship of flow rate to pressure drop experienced by the oil as it flows through the reservoir rock is influenced by the following: 1) reservoir geometry, 2) oil properties, and 3) reservoir rock properties.

3.1 Reservoir Geometry

All of the calculation procedures used in this report are based on flow systems of radial geometry, such as shown in Fig. 3.1. In this radial system

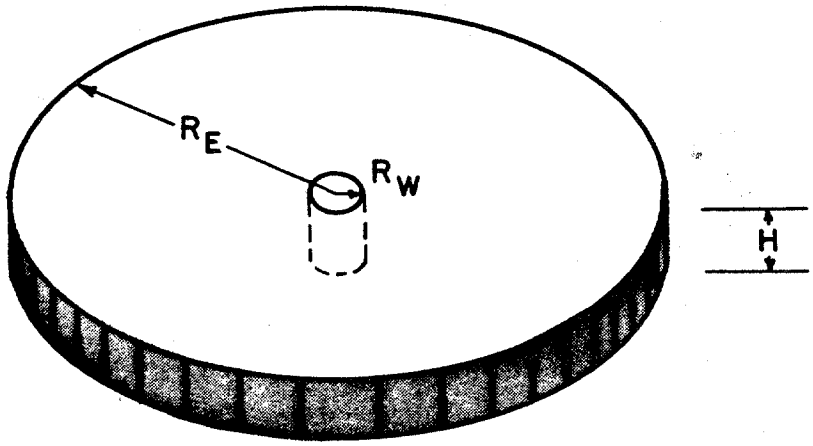

Fig. 3.1. A Radial System of Thickness h, External Radius r_e, and Wellbore Radius r_w.

r_w represents the radius of the wellbore, r_e represents the outer or external radial boundary of the reservoir, and h represents the net thickness of the formation. The value of r_w is commonly taken to be the radius of the drill bit if oil is flowing into an open hole and is taken to be the internal radius of the casing if it is flowing through perforated casing. The value of r_e is the radius of the boundary of the reservoir, if the reservoir is indeed circular. Since no reservoirs are truly radial in shape and wells may be located off center, an equivalent radius is normally used, defined as the radius of a circle whose area is the same as the reservoir. This procedure has been shown in practice to be a good approximation for most reservoir systems. If the reservoir area is in acres, the equivalent external radius r_e in feet is

$$r_e = (43{,}560 \times A/\pi)^{0.5} \qquad (3.1)$$

For an area of 125 acres, the equivalent external radius is 1316 ft.

3.2 Effect of Free Gas Presence

Once the pressure anywhere in the reservoir declines below the bubble point pressure, natural gas will evolve from solution and form a free gas saturation. This is most evident near the wellbore, where flowing pressures are lowest. Even if the average reservoir pressure is above the bubble point, it is quite possible that the pressure in the vicinity of the wellbore will be below the bubble point. As production continues, this area containing free gas will expand further and further out into the reservoir as pressures continue to decline.

In areas containing free gas, the flow of oil is restricted because of a decrease in the effective permeability to oil. Once the free gas saturation exceeds the so-called "critical" gas saturation, the effective permeability to gas becomes high enough to allow the movement of the free gas.

In summary, the reservoir can have essentially two different regimes of oil flow: one area where there is no free gas saturation and a second area where free gas exists and therefore impedes the flow of oil. As production continues, the first area shrinks as the second area expands. This complicates the procedures used to predict the relationship of flow rate and flowing bottomhole pressure.

If all pressures stay above the bubble point pressure, there is no gas saturation and relatively simple relationships of flow rate and flowing bottomhole pressure can be obtained. This may occur, for example, in a high permeability, active water drive reservoir containing highly undersaturated crude.

3.3 Steady State Flow - No Free Gas Saturation

The formula which relates the oil flow rate and the flowing bottomhole pressure for radial systems is Eq. 6.24 of Ref. 3.1.

$$Q = \frac{7.08Kh(p_e - p_w)}{\mu B_o \ln(r_e/r_w)} \qquad (3.2)$$

in which:

Q = flow rate in STB/day

K = oil permeability, darcies

h = reservoir thickness, ft

p_e = pressure at radius r_e, psia

p_w = wellbore pressure at r_w, psia

μ = oil viscosity, centipoise

B_o = oil formation volume factor, RB/STB

r_e/r_w = ratio of external radius to wellbore radius, dimensionless

Equation 3.2, a form of Darcy's Law, is commonly referred to as a steady-state equation. It assumes the maintenance of pressure at a value of p_e at the external radius r_e. Rearrangement of Eq. 3.2 shows that flow rate varies linearly with flowing bottomhole pressure.

3.4 Transient Flow - No Free Gas Saturation

The method described in the preceding section assumes that the steady-state pressure distribution is established in the reservoir in a negligible period of time. The approximate time to establish this distribution is expressed by Eq. 3.3 below. The time referred to is called the readjustment time, or the time for a reservoir to adjust to steady-state conditions following a change in flow rate (Ref. 3.2).

$$t_r = \frac{0.04\ \mu\ c\ \phi\ r_e^2}{K} \qquad (3.3)$$

in which

t_r = readjustment time, days

μ = oil viscosity, centipoise

c = average compressibility, psi^{-1}

ϕ = porosity, fraction

K = permeability, darcies

r_e = reservoir radius, ft

Equation 3.3 may also be used to calculate the transient drainage radius at any time, i.e., the radius beyond which reservoir pressure has not been appreciably changed up to that time by the blowout or other rate changes. Re-arranging Equation 3.3 yields:

$$r_e = \left(\frac{K\,t}{0.04\,\mu\,c\,\phi}\right)^{0.5}$$

This value may then be substituted for r_e in Eq. 3.2 to yield

$$Q = \frac{14.16Kh(p_e - p_w)}{\mu B_o \ln(Kt/0.04\mu c\phi r_w^2)} \qquad (3.4)$$

Equation 3.4, as a reasonable approximation to transient flow, may be used to calculate reservoir resistance curves by procedures illustrated in the following example.

3.5 Illustrative Example 3.1

Let

P_e = 5,000 psig K = 0.5 darcy μ = 0.39 cp

h = 10 ft B_o = 1.5 RB/STB r_w = 0.333 ft

$c_{avg} = 15 \times 10^{-6}\,psi^{-1}$ ϕ = 0.20

Substituting these data into Eq. 3.4 yields

$$Q = \frac{121(5{,}000 - p_w)}{\ln(9.635 \times 10^7\ t)}$$

For p_w = 3000 psig and t = 10 days

Q = 11,700 BOPD

Other values of t and p can be utilized to provide the data points for the curves on the right of Fig. 3.2 for 1, 10, and 100 days. In most blowouts neither the formation thickness nor the formation permeability is known with precision. Using Eq. 3.1 and the other data of Example 3.1 except for the formation capacity, which is reduced from 5 darcy-feet to 2.5 darcy-feet, the curves on the left of Fig. 3.2 are obtained, again for 1, 10 and 100 days.

Use of Equation 3.4 assumes that the reservoir boundary is never reached during the duration of the blowout. If the reservoir size is known, Eq. 3.3 can be used to estimate the time at which the boundary is felt. For elapsed times greater than that calculated by Eq. 3.3, the prediction of flow rate versus p should be with Eq. 3.5:

$$Q = \frac{7.08Kh(p - p_w)}{\mu B_o \ln(r_e/r_w - 0.75)} \qquad (3.5)$$

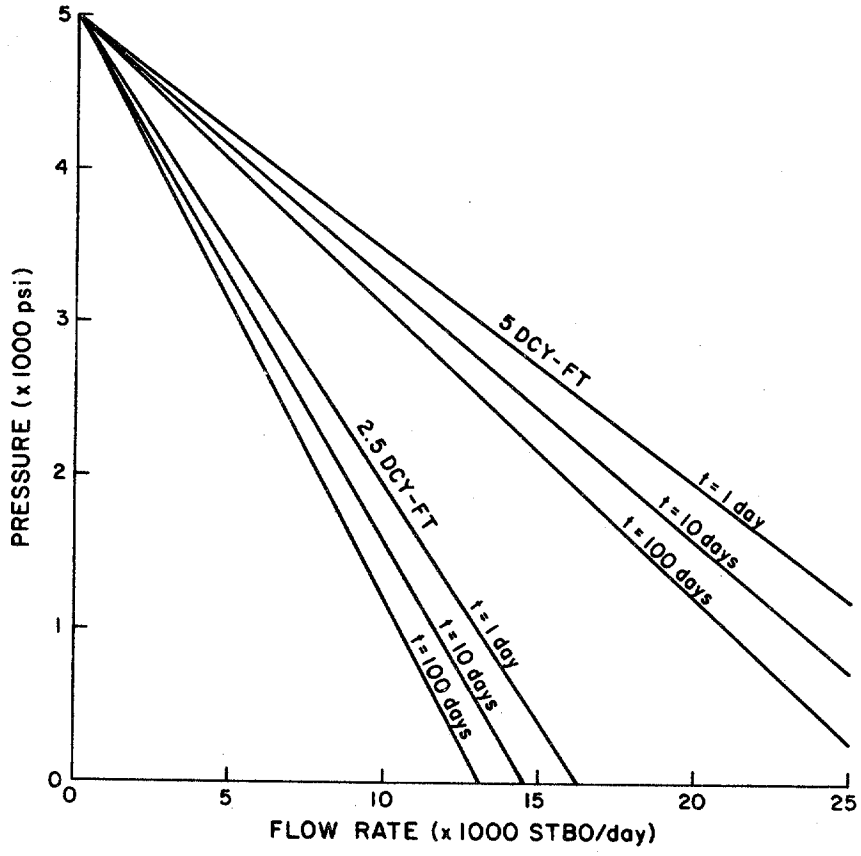

Fig. 3.2. Calculated Bottomhole Pressure as a Function of Flow Rate and Time for Illustrative Example 3.1.

where p is the average reservoir pressure and r is the equivalent reservoir boundary radius.

3.6 Flow With Free Gas Saturation Around the Wellbore

The method of the previous sections can be expected to yield meaningful results as long as the pressure throughout the reservoir remains at or above the bubble point. This could be the case for a very active water-drive reservoir. However, as reservoir pressure around the wellbore drops below the bubble point, dissolved gas comes out of solution and forms a free gas saturation. This gas saturation causes a reduction in the oil permeability and further impedes the flow of oil. As production continues, this zone of reduced oil permeability moves further and further into the reservoir.

There have been studies that have addressed this problem. Probably the more commonly used of these two methods is that of Vogel (Ref. 3.3), which states:

$$\frac{Q_o}{Q_{omax}} = 1 - \frac{0.2p_{wf}}{p_{avg}} - \frac{0.8p_{wf}^2}{p_{avg}} \qquad (3.6)$$

where:

Q_{omax} is the oil flow rate with no free gas saturation

Q_o is the oil flow rate with free gas saturation

p_{wf} is the flowing bottomhole pressure and

p_{avg} is the average reservoir pressure.

Basically, this equation states that the productivity will decrease as reservoir pressure decreases, in contrast to the methods of the previous sections, which resulted in a constant productivity. The reservoir resistance curves of Fig. 3.2 would no longer be straight lines, but would indicate a more rapid decrease in flow rate with decreasing wellbore pressure if free gas is present.

The prediction of the actual quantitative effect of the expanding gas saturation region in a blowout situation does not appear to be well defined with the hard-calculation methods in the literature intended for less drastic well behavior. Perhaps the most precise technique would use the powerful computer reservoir simulators available from the industry (Ref. 3.4). The description and use of such simulators is beyond the scope of this work.

SECTION 4

FLOW STRING RESISTANCE

4.1 Flow String Resistance Calculations

Flow string resistance for simultaneous oil, gas, and water flow can be estimated using one of the numerous correlations available for that purpose. Most of these correlations are documented in Ref. 4.1. All of these correlations are complicated and require digital computer solution.

Two-phase correlations can be loosely classified into three categories. The first category does not consider different flow regimes and assumes no slip. This is the situation when the liquid and gas travel up the well at the same velocity. An example of this type is the Poettmann and Carpenter correlation (Ref. 4.2). The second category considers slip but does not consider different flow regimes. An example of this type is the Hagedorn and Brown correlation (Ref. 4.3). The third category considers both slip and different flow regimes. An example of this type is the Beggs and Brill correlation (Ref. 4.4). Typical flow regimes in the third category are bubble flow, slug flow, transition flow, and mist flow. Correlations of the three categories will be used in the following illustrative examples.

Flow string resistance is a function of the flow path geometry. Three simplified geometries are considered in the following examples:

1. Flow up the drillpipe.

2. Flow up the drillpipe-casing annulus.

3. Flow up the casing (drillpipe out of the hole).

For all examples, it is assumed that casing has just been set and the blowout occurred shortly after drilling out of the casing. The effects of the bit, nozzles, drillcollars, tool joints, and open hole are not considered. A linear temperature gradient and a perfectly vertical well are assumed. Well data common to all examples are listed in Table 4.1.

The effects of different gas-oil ratios are shown in each example by considering gas-oil ratios of 500, 1000, 1500 and 2000 SCF/STB. A sensitivity analysis of the other various parameters is not included as this would imply an accuracy that does not exist. This lack of accuracy can be seen by the different curves that the various correlations yield for the same input data.

Table 4.1

Specific Well Data

Well depth = 10,000 ft
Static bottomhole pressure = 5000 psig
Bottomhole temperature = 200° F
Flowing surface temperature = 180° F
Oil gravity = 35° API
Gas gravity = 0.65 (air = 1)
Drillpipe = 5" O.D., 19.5#/ft (4.276" I.D.)
Casing = 10 3/4" O.D., 45.5#/ft (9.95" I.D.)

4.2 Critical Flow

At high flow rates and low pressures, critical flow can occur. This is defined as the point where the average velocity of the flowing fluids reaches the velocity of sound in the fluids. Decreases in downstream pressure will not increase the average velocity any further.

In the case of an uncontrolled blowout, the minimum pressure and, therefore, the maximum velocity would occur at the surface. As long as the velocity at atmospheric pressure is below the velocity of sound in the fluids, critical flow does not exist, and atmospheric surface pressure can be used for the surface pressure. When the exit velocity at atmospheric pressure reaches the velocity of sound in the fluids, the pressure at the point of discharge into the atmosphere is higher than atmospheric pressure. To determine this pressure, the flowing empirical equation can be used:

$$P = \frac{10 \times Q_L R_P^{0.546}}{d^{1.89}} \qquad (4.1)$$

where:

P = pressure (psia)

Q_L = liquid production rate (STB/DAY)

R_P = producing gas-liquid ratio (SCF/STB)

d = pipe diameter (64th's of an inch)

This equation was developed from empirical data on chokes. Whenever the pressure as calculated by Equation 4.1 exceeds atmospheric pressure, it should be used for the surface pressure.

4.3 Flow Up Drillpipe (Illustrative Example)

Figure 4.1 illustrates the flow path of a blowout through the drillpipe. This situation could occur when the outside blowout preventers were closed when the well kicked but for some reason the inside blowout preventer or "TIW" valve was not installed.

The bottomhole pressures for various flow rates and gas-oil ratios using the Poettmann and Carpenter, Hagedorn and Brown and Beggs and Brill correlations are tabulated in Table 4.2 and are graphed in Figures 4.2, 4.3, and 4.4 respectively. Inspection of the figures reveals that the Poettmann and Carpenter correlation indicates the lowest bottomhole pressures of the three correlations considered. This would result in the Poettmann and Carpenter correlation indicating higher flow rates than the other correlations when cross plotted with formation resistance as discussed in Section 5. The Beggs and Brill correlation indicates higher bottomhole pressures and, therefore, lower flowrates than the other two correlations. The Beggs and Brill correlation also seems to be more sensitive to gas-oil ratio than the other correlations.

4.4 Flow Up the Drillpipe-Casing Annulus (Illustrative Example)

Fig. 4.5 illustrates the flow path of a blowout up the drillpipe-casing annulus. This situation occurs where the outside blowout preventers either failed or were not closed while flow up the drillpipe was prevented by a float or an inside blowout preventer.

The bottomhole pressures for various flow rates and gas-oil ratios using the Poettmann and Carpenter, Hagedorn and Brown, and Beggs and Brill correlations are tabulated in Table 4.3 and are graphed in Figures 4.6, 4.7, and 4.8 respectively.

Once again, the Beggs and Brill correlation was more sensitive to gas-oil ratio and yielded lower flow rates than the Poettmann and Carpenter and Hagedorn and Brown correlations. It should be noted that unlike the Hagedorn and Brown and the Beggs and Brill correlations, the Poettmann and Carpenter correlation does not handle annular flow any differently than pipe flow. To obtain the desired pressures, Poettmann and Carpenter use an "equivalent diameter" i.e., a pipe diameter whose cross-sectional area equals that of the annulus. In annular flow, however the wetted perimeter is much greater than the equivalent pipe diameter. Hence the friction effect will be underestimated. The result is that for annular flow the Poettmann and Carpenter correlation yields pressures that are too low and flow rates that are too high.

Table 4.2

Bottomhole Pressure for Flow Up Drillpipe

Q_o	GOR (SCF/STB)			
STB/day	500	1000	1500	2000
Poettmann and Carpenter				
10,000	1428	1107	1116	1184
15,000	1951	1627	1660	1772
20,000	2416	2121	2191	2350
25,000	2823	2595	2708	2911
Hagedorn and Brown				
10,000	2107	1751	1759	1843
15,000	2733	2436	2510	2657
20,000	3295	3142	3295	3527
25,000	2829	2880	4133	4468
Beggs and Brill				
10,000	2723	2500	2558	2724
15,000	3292	3270	3487	3744
20,000	3823	4068	4404	4820
25,000	4350	4813	5367	5940

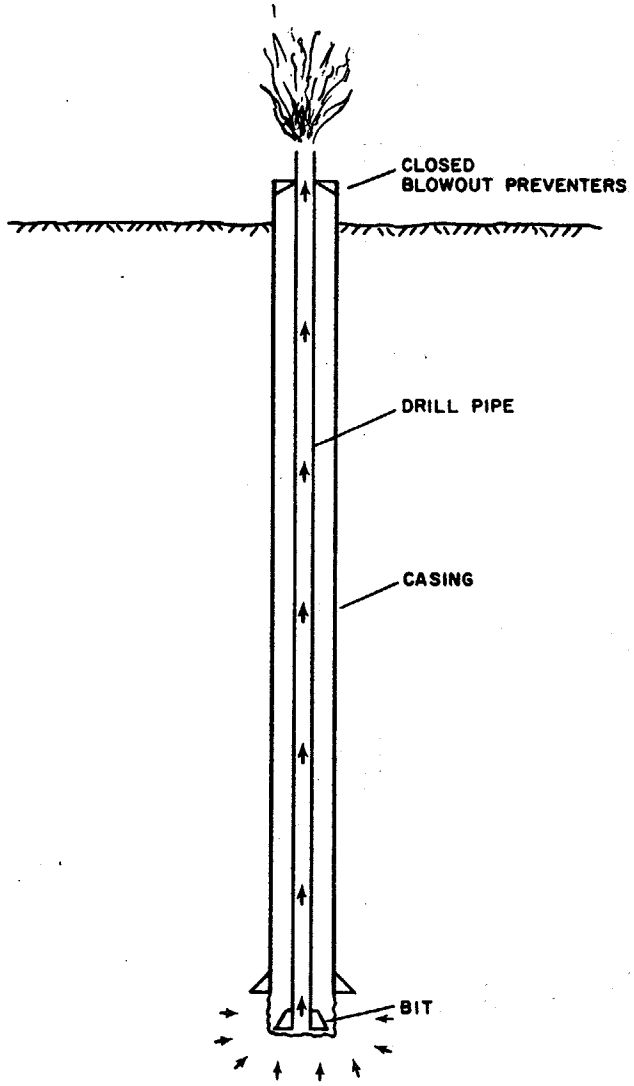

Fig. 4.1. Illustrated of Uncontrolled Blowout Up the Drillpipe.

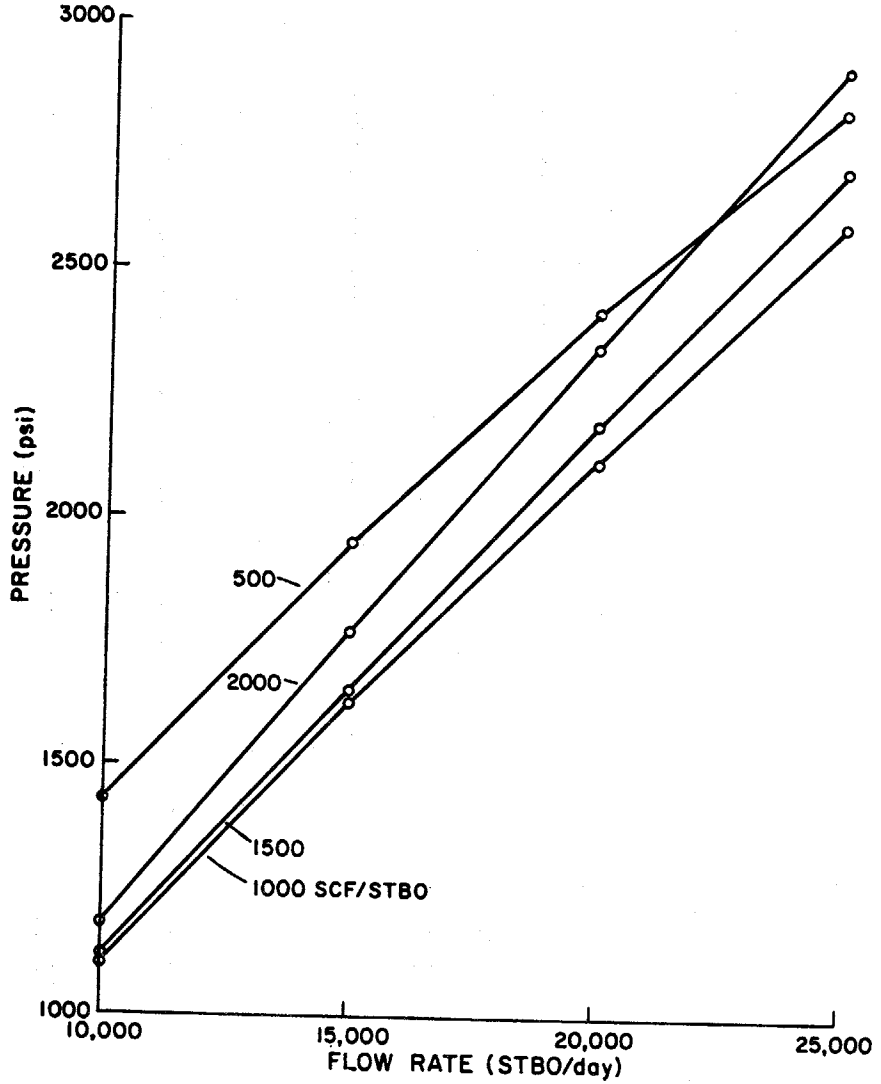

Fig. 4.2. Pressure at 10,000 ft. as a Function of GOR and Flow Rat. Poettmann and Carpenter Correlation. Flow Up Drillpipe.

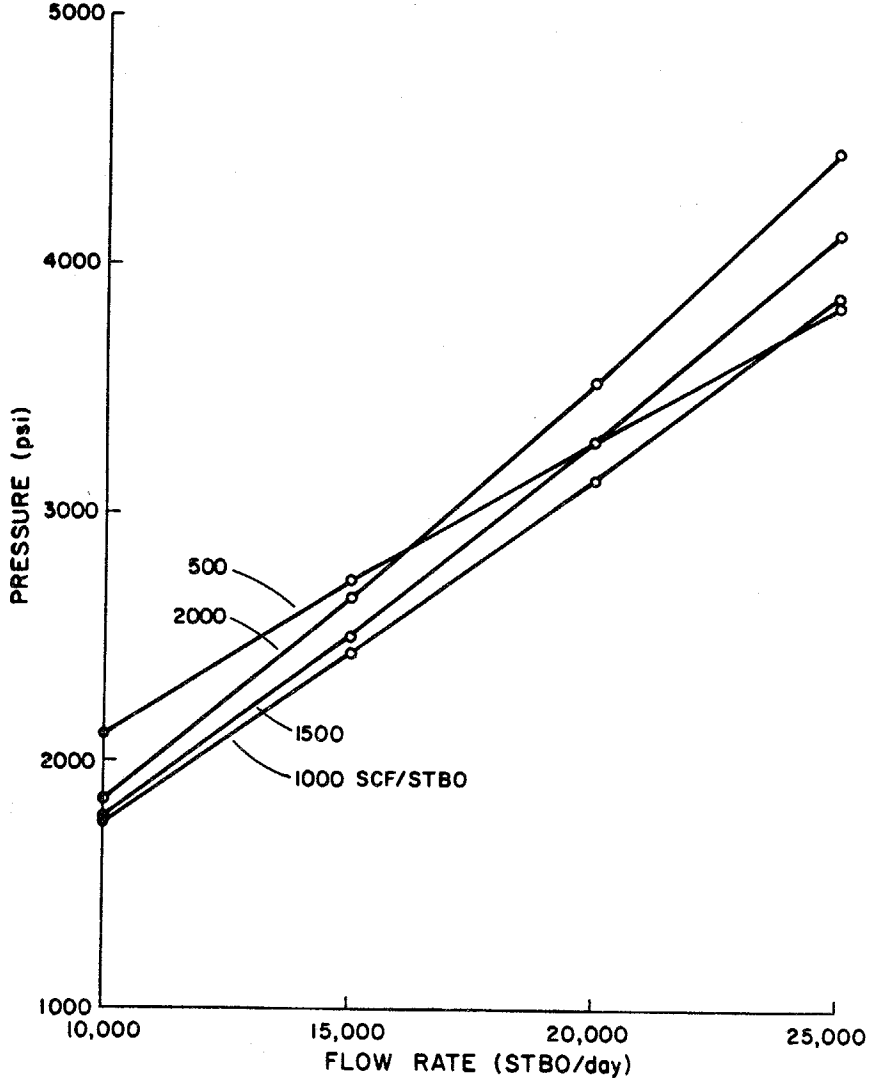

Fig. 4.3. Pressure at 10,000 ft. as a Function of GOR and Flow Rate. Hagedorn and Brown Correlation. Flow Up Drillpipe.

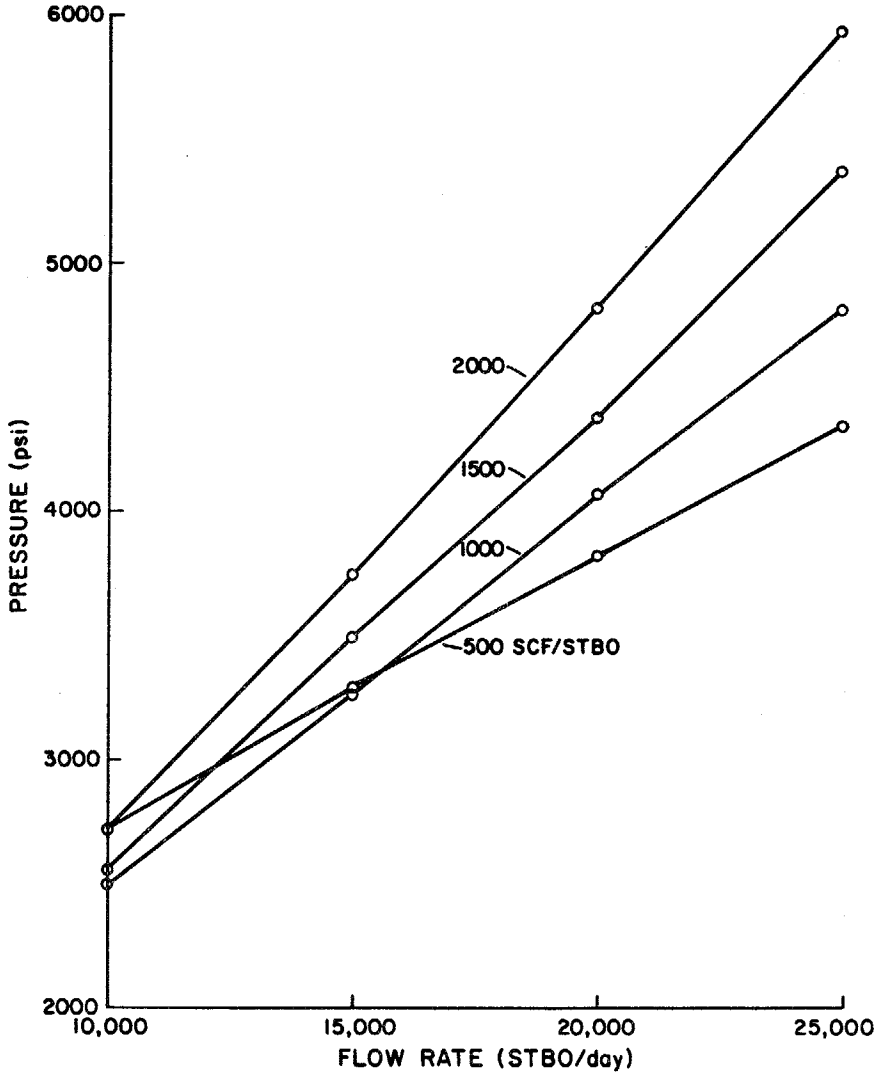

Fig. 4.4. Pressure at 10,000 ft. as a Function of GOR and Flow Rate Beggs and Brill Correlation. Flow Up Drillpipe.

Table 4.3

Bottomhole Pressure for Flow Up Annulus

Q_o	GOR (SCF/STB)			
STB/day	500	1000	1500	2000
Poettmann and Carpenter				
10,000	442	279	262	264
20,000	623	405	397	418
30,000	896	615	607	641
40,000	1150	825	817	862
Hagedorn and Brown				
10,000	813	532	486	458
20,000	1126	790	770	779
30,000	1383	1035	1018	1059
40,000	1649	1282	1271	1333
Beggs and Brill				
10,000	1561	1021	836	760
20,000	1794	1365	1268	1265
30,000	2056	1692	1653	1682
40,000	2323	1974	1968	2063

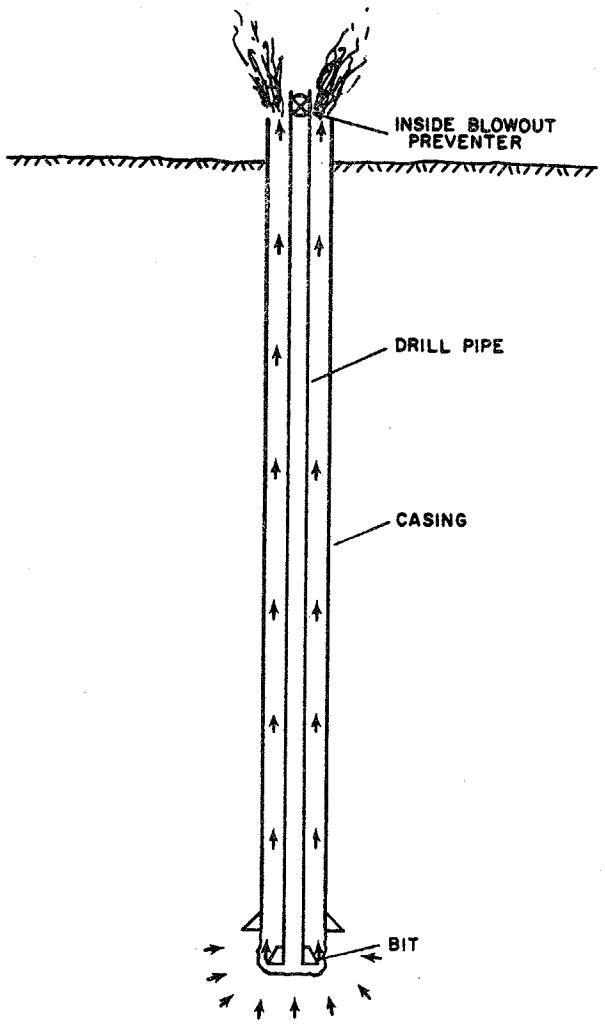

Fig. 4.5. Illustration of Uncontrolled Blowout Up the Drillpipe-Casing Annulus.

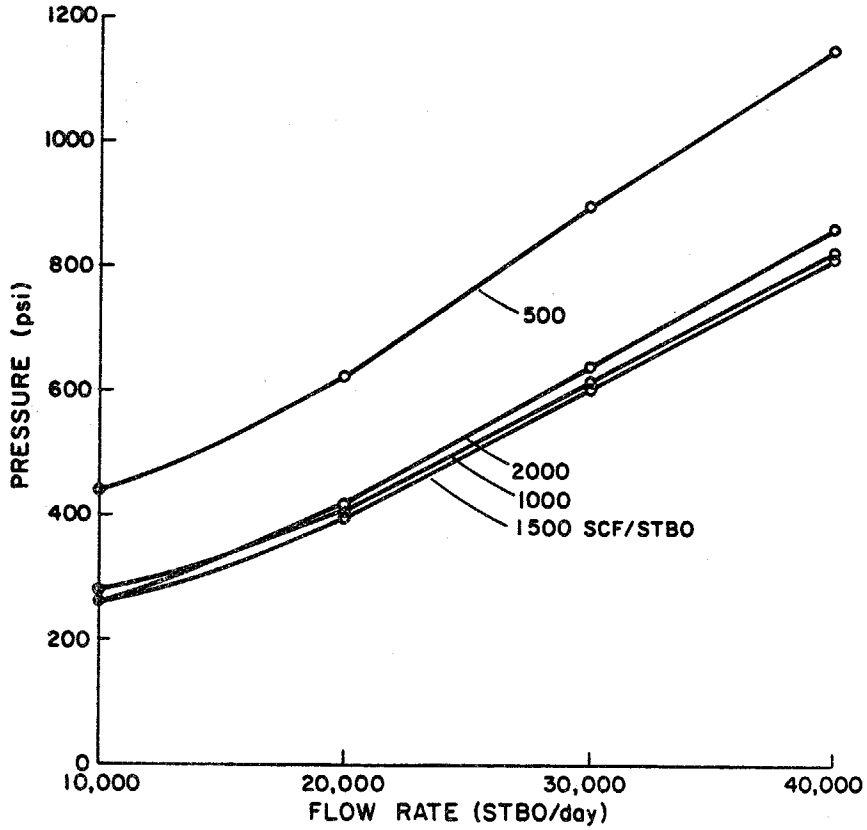

Fig. 4.6. Pressure at 10,000 ft. as a Function of GOR and Flow Rate. Poettman and Carpenter Correlation. Flow Up Annulus.

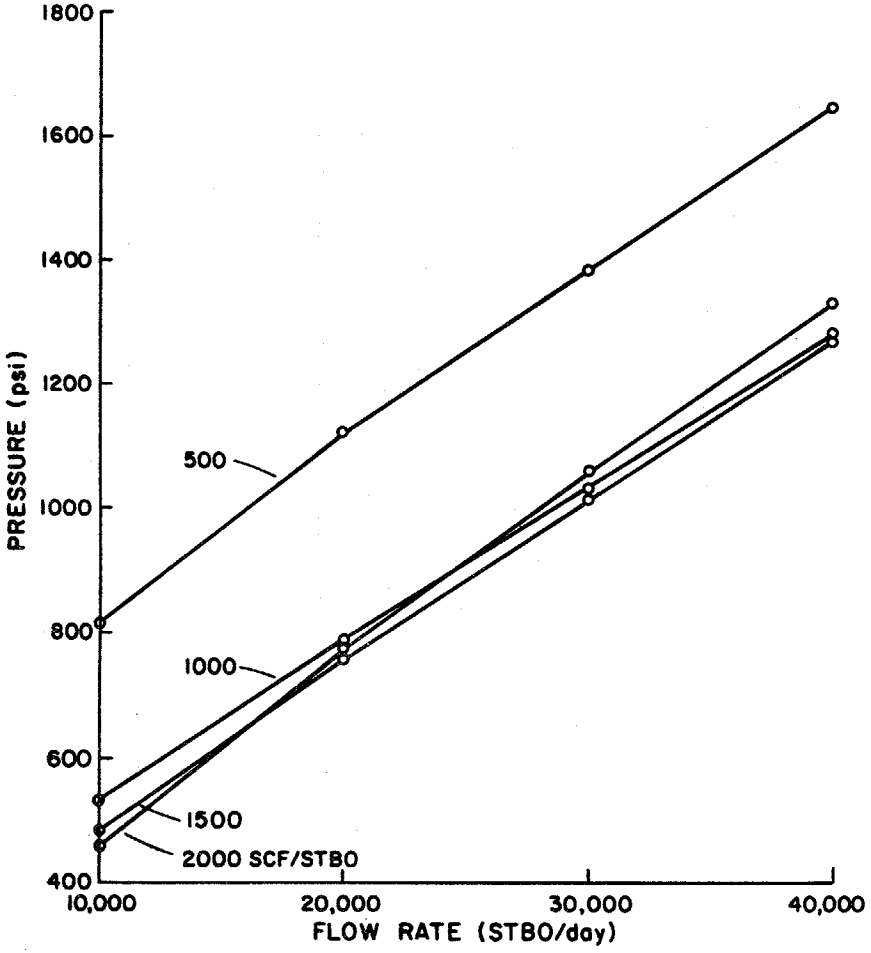

Fig. 4.7. Pressure at 10,000 ft. as a Function of GOR and Flow Rate. Hagedorn and Brown Correlation. Flow Up Annulus.

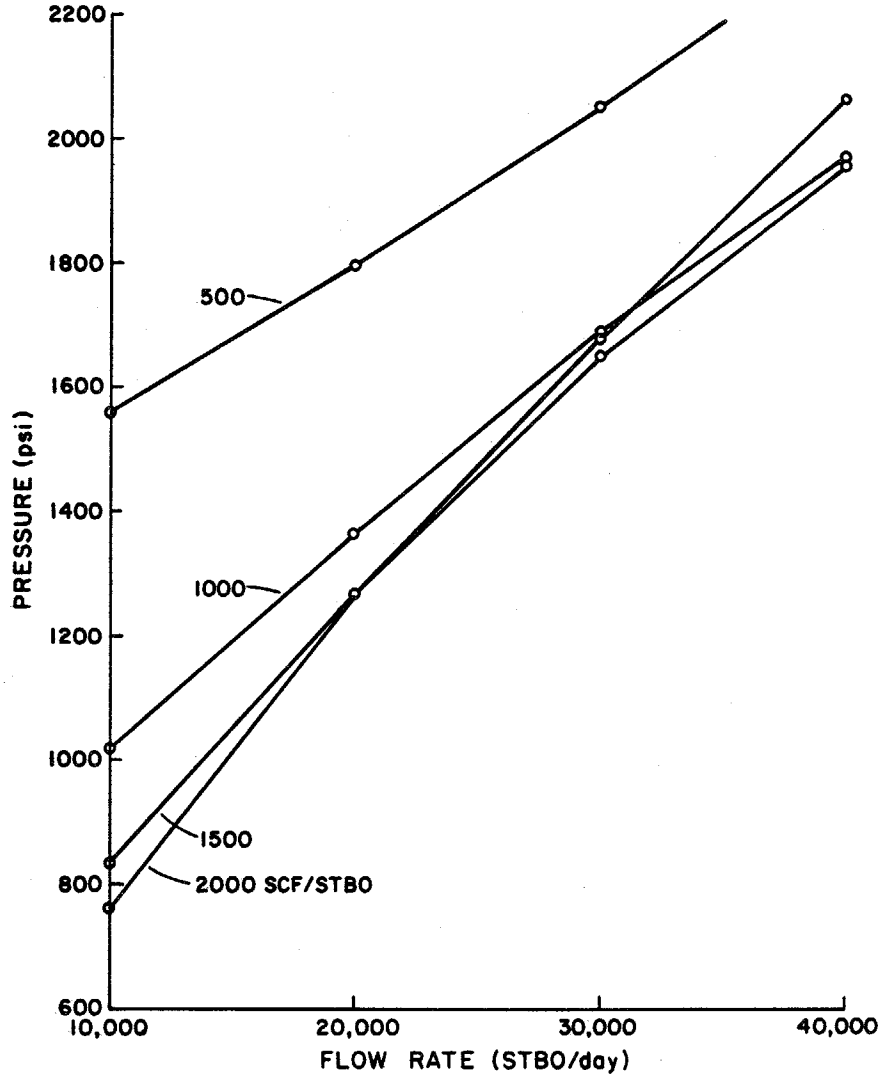

Fig. 4.8. Pressure at 10,000 ft. as a Function of GOR and Flow Rate. Beggs and Brill Correlation. Flow Up Annulus.

4.5 Flow Up the Casing (Illustrative Example)

Fig. 4.9 illustrates the flow path of a blowout up the casing with the drillpipe out of the hole. This situation would most likely occur if the hole were not filled during a trip out of the hole, and a kick was taken when the drillpipe was completely out of the hole.

The bottomhole pressures for various flowrates and gas-oil ratios using the Poettmann and Carpenter, Hagedorn and Brown, and Beggs and Brill correlations are tabulated in Table 4.4 and are graphed in Figures 4.10, 4.11, and 4.12 respectively. As before, the Beggs and Brill correlation appears more sensitive to gas-oil ratio and yields lower flow rates than the Poettmann and Carpenter and Hagedorn and Brown correlations.

Table 4.4

Bottomhole Pressure for Flow Up Casing

Q_o	GOR (SCF/STB)			
STB/Day	500	1000	1500	2000
Poettmann and Carpenter				
10,000	347	214	200	202
20,000	466	287	278	292
30,000	665	432	422	445
40,000	862	583	571	603
Hagedorn and Brown				
10,000	641	410	367	346
20,000	916	611	584	566
30,000	1124	782	757	777
40,000	1307	945	916	963
Beggs and Brill				
10,000	1514	908	685	585
20,000	1629	1140	993	941
30,000	1796	1384	1272	1266
40,000	1980	1587	1513	1546

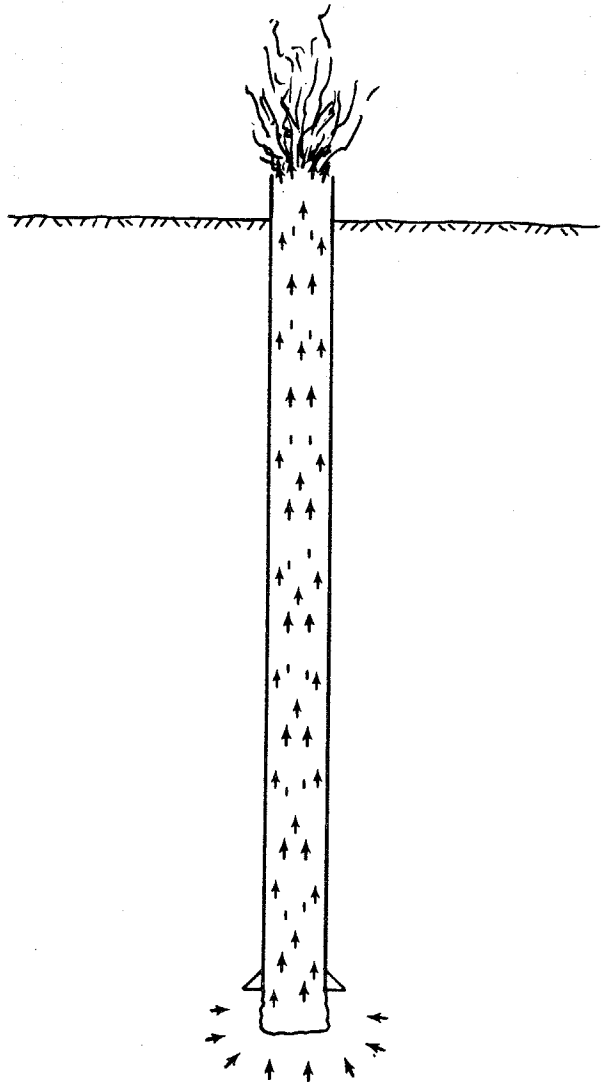

Fig. 4.9. Illustration of an Uncontrolled Blowout Up the Casing. (Drill-pipe Out of the Hole.)

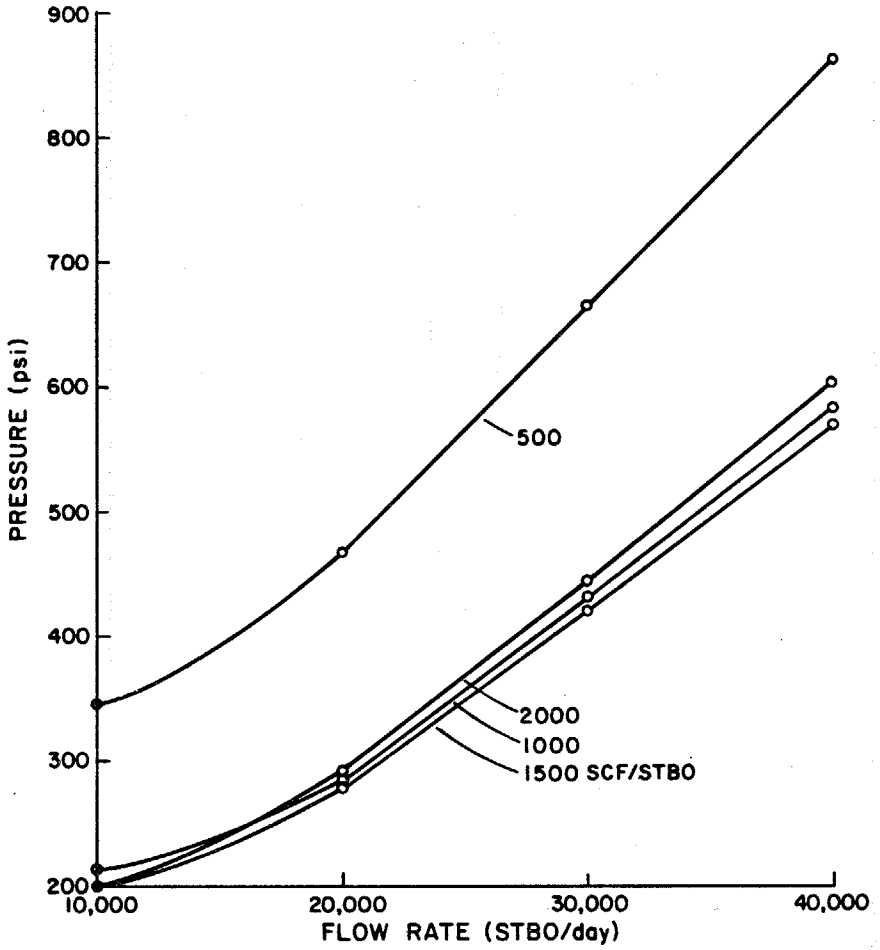

Fig. 4.10. Pressure at 10,000 ft. as a Function of GOR and Flow Rate. Poettman and Carpenter Correlation. Flow Up Casing.

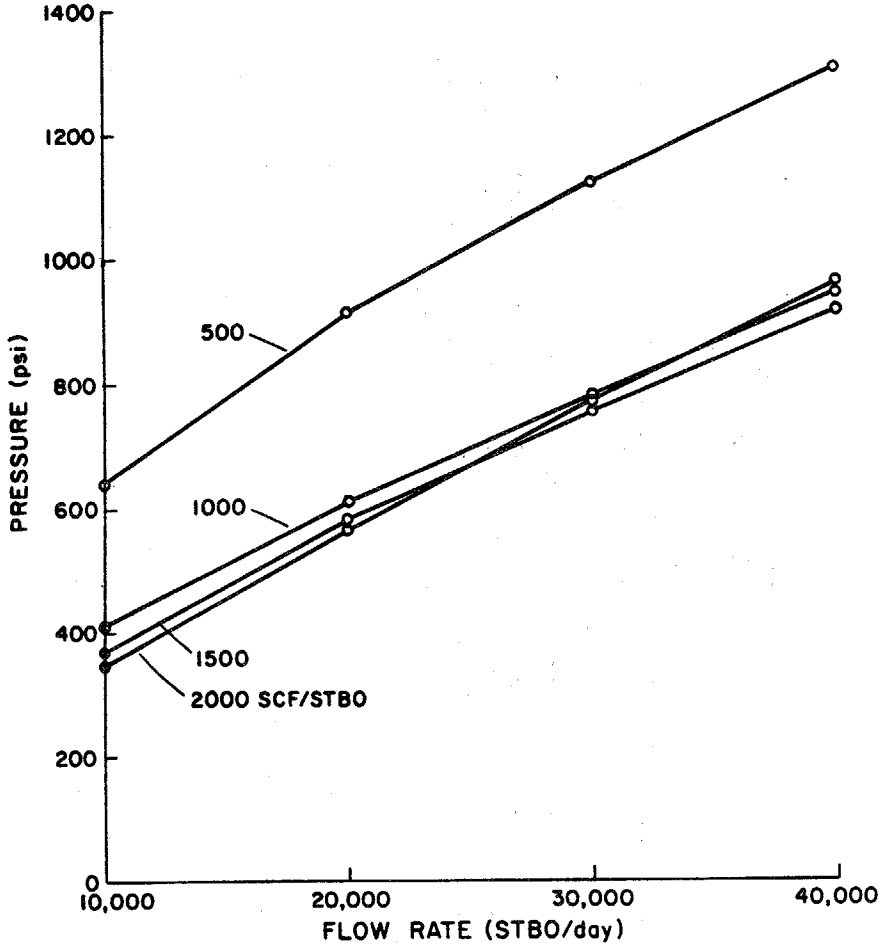

Fig. 4.11. Pressure at 10,000 ft. as a Function of GOR and Flow Rate. Hagedorn and Brown Correlation. Flow Up Casing.

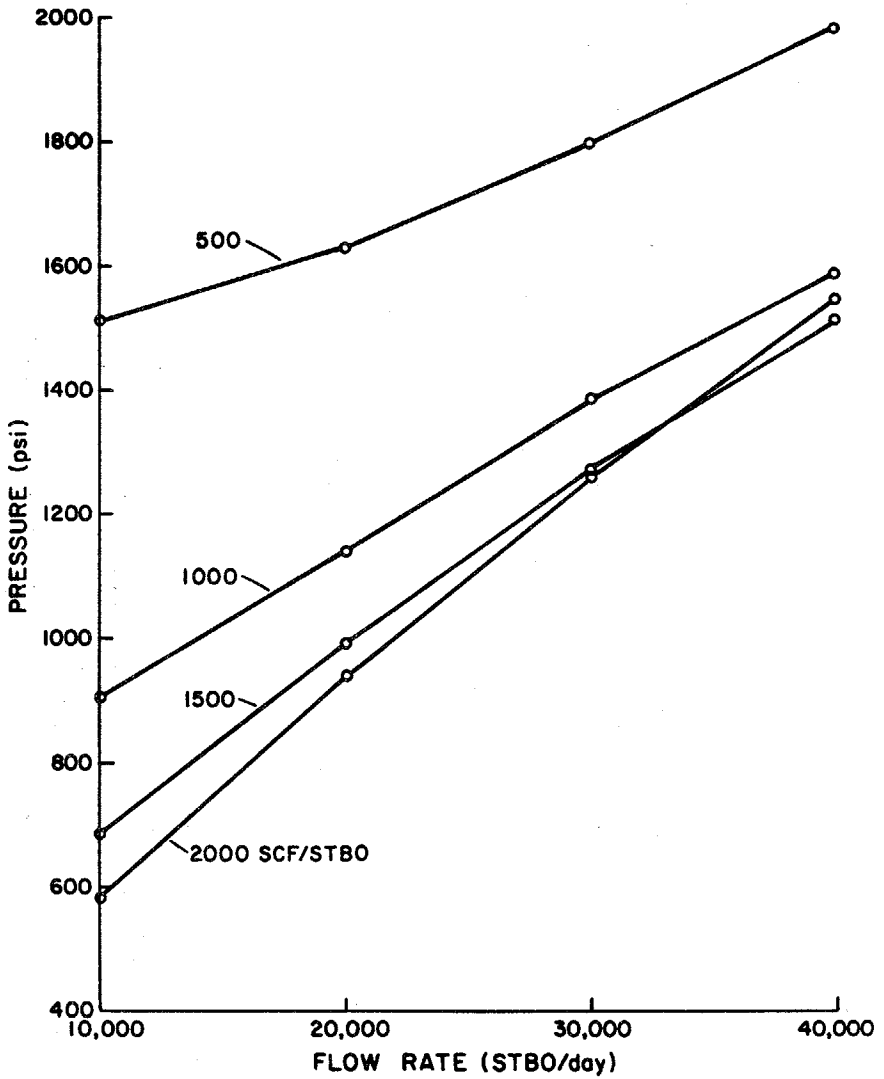

Fig. 4.12. Pressure at 10,000 ft. as a Function of GOR and Flow Rate. Beggs and Brill Correlation. Flow Up Casing.

4.6 Limitations and Accuracy of Flow String Resistance Calculations

Most of the parameters required to calculate flow string resistance can be measured or estimated with fair accuracy. Unfortunately, the various correlations do not yield the same values for flow string resistance. This is illustrated in Fig. 4.13 which compares the results of the three correlations considered for the case of flow up the drillpipe-casing annulus with a gas-oil ratio of 1000 SCF/STB. The figure indicates that the results will be highly dependent upon the correlation used.

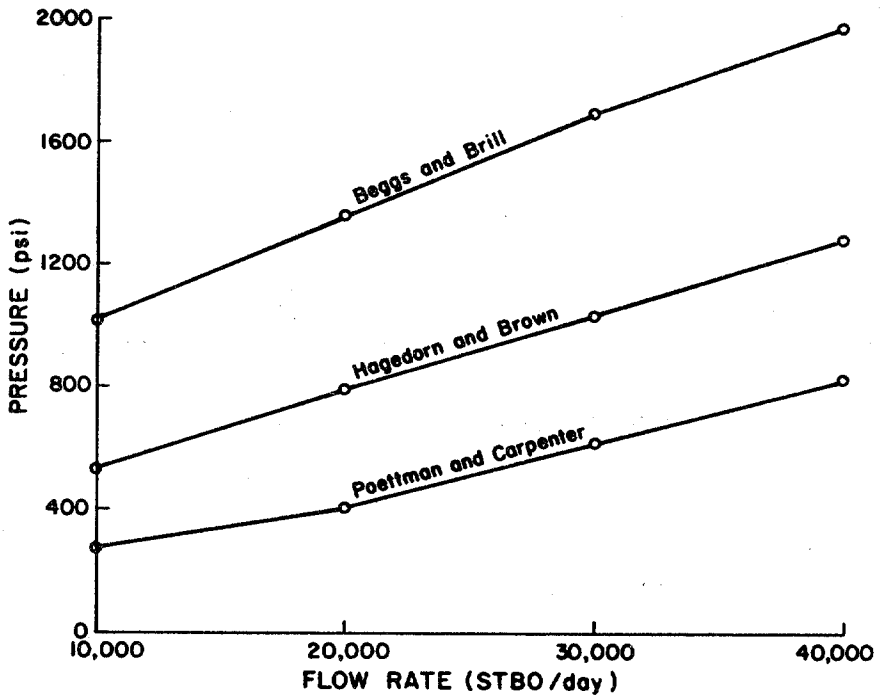

Fig. 4.13. Comparison of Multi-Phase Flow Correlations. Flow Up Annulus. GOR = 1000 SCF/STBO

Except for gas-oil ratio, a sensitivity analysis of the various input parameters was not performed. This was avoided because it would imply an accuracy which does not exist. The effects of gas-oil ratio were included because changes in gas-oil ratio affect the mass flow rate. The large effect of gas-oil ratio on flow string resistance can be seen in most of the preceding graphs.

The surface pressure for critical flow as calculated by Eq. 4.1 is of unknown accuracy. The equation was developed from empirical data on chokes and its extension to large diameters and flowrates is beyond the conditions for which the correlation was developed. Further research in this area is certainly needed.

In general, the procedure followed in this study could be easily extended to a specific well with a more complicated well geometry. The procedure should be able to yield "order of magnitude" values of flow rate if reasonably accurate information is available.

SECTION 5

CROSS PLOTS OF FORMATION AND FLOW STRING RESISTANCE

Flow string resistance and formation resistance control the amount of oil escaping during a blowout. Formation resistance occurs as oil flows through the small, tortuous pore spaces of the reservoir rock toward the wellbore. Flow string resistance occurs as oil flows up the wellbore toward the surface. These two resistances act in series, and it cannot be said which is dominant.

Techniques are available to estimate the relationship of the flow rate of the escaping oil to these two resistances. The procedure follows three basic steps:

1. FORMATION RESISTANCE

   Using an appropriate formula for the flow of oil in the reservoir, the flow rates are calculated for a range of flowing bottomhole pressures. A plot of these data, such as shown in Fig. 3.2, is an expression of the formation resistance, which involves properties of the reservoir rock and oil. As indicated, maximum flow rate occurs for zero bottom hole pressure, and the rate declines as bottomhole pressure rises.

2. FLOW STRING RESISTANCE

   Using appropriate multiphase flow correlations for the flow of oil through pipes, annuli, etc., a flow rate is assumed. Using a surface flowing pressure, usually determined by sonic or critical flow at the surface, the corresponding pressure is calculated at the bottom of the flow string. Other bottom hole pressures are calculated for a range of assumed flow rates, the results of which can be plotted, as in Fig. 4.13.

3. BLOWOUT RATE

   The intersection of the formation and flow string resistance curves is the calculated blowout rate. An example of this can be seen in Fig. 5.1. The formation resistance curves are from Fig. 3.2 (illustrative example 3.1), and the flow string resistance curves are from Fig. 4.13. The intersections of curves indicate flow rate.

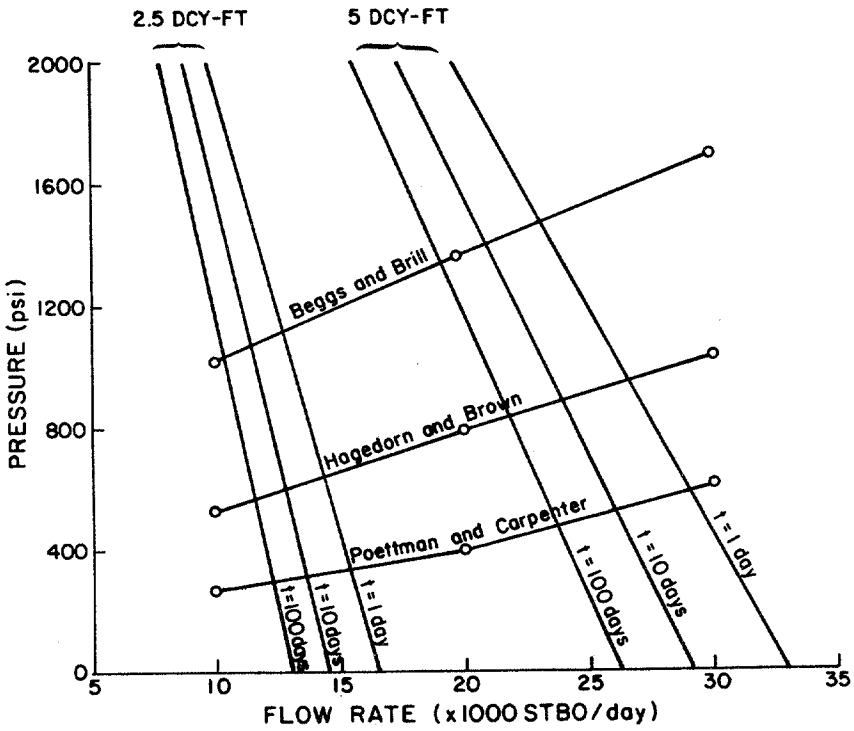

Fig. 5.1. Crossplot of Formation and Flowstring Resistance.

As can be seen from Fig. 5.1, the flowrate is highly dependent on the multiphase flow correlation used. For example, a production time of 10 days and formation capacity of 5 darcy-ft indicate flow rates of about 21,100 STBO/day from the Beggs and Brill correlation, 24,000 STBO/day from the Hagedorn and Brown correlation, and 26,100 STBO/day from the Poettmann and Carpenter correlation. Of the three correlations considered, the Poettmann and Carpenter correlation is the least accurate in annular flow, so a best estimate of the flow rate would be in the range of 21,100 to 24,000 STBO/day.

Fig. 5.1 also shows that the flow rate is directly proportional to the formation capacity. If the range of the estimated formation capacity is 2.5 to 5.0 darcy-ft, the best estimate of the flow rate would be in the range of 11,500 to 24,000 STBO/day.

SECTION 6

SUGGESTIONS FOR FURTHER INVESTIGATION

The foregoing sections have presented the state of the art for determining gas flow rates and vented volumes during blowouts. Such presentations naturally evoke thought on further work which might improve the determinations. Suggestions for further work are of two kinds: those which seek to improve or refine current technology and those which propose new technology, either innovative or adapted from other areas of technology.

6.1 Refinements in Current Technology

The methods presented in this report are extensions of solutions to common engineering problems. The precision of the formation resistance calculations as applicable to the oil well blowout problem is more than adequate because of the unavailability and/or imprecision of most of the data. Improvements in estimating the formation resistance are therefore not needed.

On the contrary, the precision of the bleedline and flow string resistance calculations are not known. These calculations are based on two-phase and critical-flow correlations that were developed for flow rates and flow path sizes that are much smaller than would be encountered in an oilwell blowout. While the available correlations are sufficiently precise in the ranges for which they were developed, their precision when applied to an oilwell blowout is unknown. For this reason, verification of the existing correlations or development of new correlations is needed. New correlations are also needed for the case of gas-condensate wells.

6.2 Suggestions for New Technology

Several different methods for measuring vented volumes during oilwell blowouts should be considered for further study and were discussed in an earlier report (Ref. 6.1). These include measuring heat flux from a burning blowout and dividing it by the estimated heating value to determine flow rate, measurement of the angular deflection of a bullet shot through the blowout stream, sensing elements placed in the blowout stream, measurement of the size and shape of an ignited blowout, measurement of the level and frequency of the sounds emitted by a blowout, and the measurement of air velocities and pressures near the blowout. Of course, the volume of oil can be estimated from the areal extent and thickness of an oil slick, if reasonable corrections for weathering of the oil can be made. Adequate technology for these techniques is not presently available.

References

1.1 Bassiouni, Z. et al.: "Methods for Determining Vented Volumes During Gas Well Blowouts," DOE/BETC/2215-1, published by U.S. Department of Energy (October, 1980).

1.2 Sims, W. P. and W. G. Frailing: "Lakeview Pool, Midway-Sunset Field," Trans AIME (1950) 189, 7.

1.3 "Pemex Claims 1 Ixtoc Oil Flow Cut to 10,000 b/d," Oil and Gas Journal - August 20, 1979, page 62.

2.1 "API Recommended Practices for Blowout Prevention," American Petroleum Institute, API RP 53 (February, 1976).

2.2 Beggs, H. D. and J. P. Brill: "A Study of Two-Phase Flow in Inclined Pipes," Trans AIME (1973), 607.

2.3 Dukler, A. E. et al.: "Gas-Liquid Flow in Pipelines, I. Research Results," AGA-API Project NX-28 (May, 1969).

2.4 Eaton, B. A.: "The Prediction of Flow Patterns, Liquid Holdup, and Pressure Losses Occurring During Continuous Two-Phase Flow in Horizontal Pipelines," Ph.D. Dissertation, The University of Texas at Austin (1965).

2.5 Lockhart, T. W. and R. C. Martinelli: "Proposed Correlation of Data for Isothermal Two-Phase, Two Component Flow in Pipes," Chem. Eng. Prog. (January, 1949) 39.

2.6 Brill, J. P. and H. D. Beggs: Two-Phase Flow in Pipes, published by the University of Tulsa (1978).

2.7 Gilbert, W. E.: "Flowing and Gas-Lift Well Performance," API Drilling and Production Practices (1954) 126.

2.8 Crane Company: "Flow of Fluids Through Valves, Fittings, and Pipes," Technical Paper 410.

3.1 Craft, B. C. and M. F. Hawkins: Applied Petroleum Reservoir Engineering, Prentice-Hall, Inc., Englewood Cliffs, N.J. (1959) 284.

3.2 Ibid., 289.

3.3 Vogel, J. V.: "Inflow Performance Relationship for Solution Gas Drive Wells," J. Pet. Tech. (January, 1968) 83-93.

3.4 Scientific Software Corporation: Black Oil Simulation System "BOSS" User's Guide.

4.1 Brill, J. P. and H. D. Beggs: Two-Phase Flow in Pipes, published by the University of Tulsa (1978).

4.2 Poettmann, F. H. and P. G. Carpenter: "The Multiphase Flow of Gas, Oil, and Water Through Vertical Flow Strings with Application to the Design of Gas-Lift Installations," Drill. and Prod. Prac., API (1952) 257-317.

4.3 Hagedorn, A. R. and K. E. Brown: "Experimental Study of Pressure Gradients Occurring During Continuous Two-Phase Flow in Small-Diameter Vertical Condruits," J. Pet. Tech. (April, 1965) 475-484.

4.4 Beggs, H. D. and J. P. Brill: "A Study of Two-Phase Flow in Inclined Pipes," Trans AIME (1973) 607.

4.5 Gilbert, W. E.: "Flowing and Gas-Lift Well Performance," API Drilling and Production Practices (1954) 126.

6.1 Bassiouni, Z. et al.: "Methods for Determining Vented Volumes During Gas Well Blowouts," published by U.S. Department of Energy (October, 1980).

☆U.S. GOVERNMENT PRINTING OFFICE: 1981-740-145/2451